

## Hybrid simulations of whistler waves generation and current closure by a pulsed tether in the ionosphere

C.L. Chang, A.S. Lipatov, A.T. Drobot, K. Papadopoulos, and P. Satya-Narayana

Science Applications International Corporation, McLean, Virginia

**Abstract.** The dynamic response of a magnetized collisionless plasma to an externally driven, finite size, sudden switch-on current source across the magnetic field has been studied using a two dimensional hybrid code. It was found that the predominant plasma response was the excitation of whistler waves and the formation of current closure by induced currents in the plasma. The results show that the current closure path consists of: a) two antiparallel field-aligned current channels at the end of the imposed current sheet; and b) a cross-field current region connecting these channels. The formation of the current closure path occurred in the whistler timescale much shorter than that of MHD and the closure region expanded continuously in time. The current closure process was accompanied by significant energy loss due to whistler radiation.

### Introduction

Determination of the dynamic response of a magnetized collisionless plasma to an "externally imposed" cross-field current or current source driven by an electromotive force (emf), is of paramount importance in space plasma physics. Of particular interest is the formation of the closure path of the induced current flow through the magnetoplasma. A quantitative description of the current closure is required to address a diverse range of space plasma physics problems, such as, the operational characteristics of emf inducing tethered systems [Colombo et. al., 1974], the efficiency of generation of ELF waves by ionospheric heating [Papadopoulos et. al., 1990], the structure of tangential discontinuities in the magnetosphere [Chapman and Ferraro, 1931], and the effect of whistler waves in the magnetotail equilibrium [Kokubun et. al., 1992].

Previous theoretical studies on the subject of current closure assumed steady state conditions and used the MHD equations [Drell et. al., 1965; Dobrowolny and Veltri, 1986]. When the steady state MHD theory is applied to the closure problem of a tethered satellite system (TSS) carrying a motionally induced emf current, it predicts a global closure path through the conducting lower ionosphere mediated by the propagation of low frequency Alfvén waves [Banks et. al. 1981]. Implicit in such formulations is the assumption that the ion polarization current is the dominant cross-field current. For this to happen the timescale must be longer than the ion cyclotron period ( $t > 1/f_{ci}$ ), so that the ions are magnetized and the electron Hall current is balanced by an opposite ion Hall current. However, processes with timescales shorter than ion cyclotron period can also contribute significantly to the current closure around TSS. For instance, there are whistler waves supported by the electron Hall current [Stenzel and Urrutia, 1990]. Distinction in timescales between the whistler and the Alfvén processes can be made analytically by considering the magnetic equation

$$\partial^2 B/\partial t^2 + \nabla \times [ \nabla \times (\partial B/\partial t) \times (cB_0/4\pi en_0) ] - v_a^2 \nabla \times [ b_0 \times (b_0 \times (\nabla \times B)) ] = 0 ; \quad (1)$$

where  $v_a$  is the Alfvén velocity,  $n_0$  is the plasma density, and  $b_0$  is the unit direction along  $B_0$ . From this equation, we can see that the second term corresponds to whistler waves and the third term corresponds to Alfvén waves. If we were to normalize Eq. (1) in such a way that  $T = f_{ci}t$  and  $X = x f_{ci}/v_a$ , then the equation depends only on dimensionless variables  $X$  and  $T$  and has no numerical coefficients. The characteristic distinction between the Alfvén and the whistler terms is determined by the timescale  $T$ . Consequently, for  $T > 1$  (or  $t > 1/f_{ci}$ ), the Alfvén wave dominates. For  $T < 1$  (or  $t < 1/f_{ci}$ ), the whistler wave dominates. In situations when the tether current is pulsed with timescale shorter than  $1/f_{ci}$ , or the transit time of the tether is of the order of msec in the Low Earth Orbit (LEO), one would expect that "local" current closure by whistler waves around TSS precedes Alfvén closure. Recent laboratory experiments indicate that this is the case. Briefly, the experiments of Stenzel and Urrutia [1990, see also Urrutia and Stenzel, 1990] studied the generation and the propagation of electromagnetic disturbances induced by a pulsed current wire in a plasma chamber with a dc magnetic field. The timescale of the current pulse favored whistler excitation. Probe measurements showed that current carrying disturbances were emitted from the current wire at approximately the group speed of a "whistler" wave packet. The dispersion characteristics and the polarization of the generated waves were those of whistlers. The propagation front carried a cross-field "polarization" current which is opposite to the imposed current in the tether wire. And most notably, the current closure was local rather than global.

These results indicate that a proper theoretical analysis of the current closure problem requires the solution of an initial value, rather than a steady state, problem, and a plasma model that includes the electron dynamic response. It is the objective of this letter to present the results of a study of the dynamic response of a two dimensional (2D) magnetoplasma to an externally imposed current source of the form

$$J_s(x,t) = I_0 \delta(z) [1 - \eta(|x| - L_s/2)] \eta(t) \hat{e}_x \quad (2)$$

where  $z$  is the direction of the magnetic field,  $x$  is the direction of the current flow,  $I_0$  is the current strength,  $L_s$  is the length of current source along  $x$ ,  $\delta$  is the Kronecker-delta function, and  $\eta$  is the step function.

### Two Dimensional Hybrid Simulations

The study has been conducted using a 2D hybrid simulation code [Mankofsky et. al., 1987]. Particular emphasis is placed upon the determination of the dynamics, the asymptotic state, and the establishment timescale of the resultant current path. It is worthwhile to discuss the validity of two commonly adopted assumptions in the hybrid simulation technique. The assumption of massless electrons implies timescales longer than the electron gyrotime  $1/f_{ce}$ , and is valid for wavelengths longer than  $c/f_{pe}$ , where  $f_{ce}$  and  $f_{pe}$  are electron gyrofrequency and plasma frequency in Hz, respectively. For parallel whistler propagation, the difference between a massless electron dispersion  $k_z =$

Copyright 1994 by the American Geophysical Union.

Paper number 94GL00700  
0094-8534/94/94GL-00700\$03.00

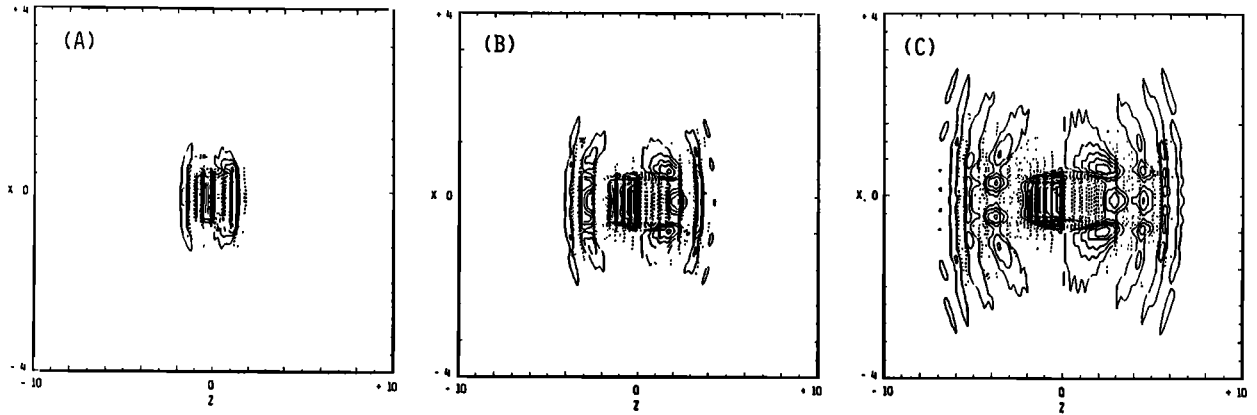


Figure 1. Contour of  $B_y$  at times: (a) 0.1 msec, (b) 0.25 msec, and (c) 0.4 msec after tether current switch-on.

$2\pi(f_{pe}/c)(f/f_{ce})^{1/2}$ , where  $k_z$  is the parallel wavenumber and  $f$  is the wave frequency in Hz, and a dispersion with finite electron mass  $k_z = 2\pi(f_{pe}/c)(f/(f_{ce}-f))^{1/2}$  becomes significant only when the wave frequency approaches the electron gyrofrequency [Helliwell, 1965]. Another assumption is the neglect of the displacement current in Ampere's law. This too, can be justified by the fact that the displacement current term does not contribute significantly to the whistler dispersion as long as  $f \ll f_{ce}$ .

The simulation was conducted for parameters relevant to TSS experiments in the F-region of the magnetosphere. The ambient magnetic field  $B_0$  and the plasma density  $n_0$  were uniform, with values equal 0.3 gauss and  $10^5$  /c.c., respectively, corresponding to an electron gyrofrequency  $f_{ce} = 0.84$  MHz and a plasma frequency  $f_{pe} = 2.84$  MHz. The ambient plasma consisted of cold oxygen ions (with realistic mass) and warm electrons at a temperature of  $T_e = 0.1$  eV. The simulation box was in the  $x$ - $z$  plane and covered a region of  $L_x = 8$  km by  $L_z = 20$  km in size. The grid resolution was 80 (in  $x$ ) by 200 (in  $z$ ) cells, which corresponds to spatial resolution of 0.1 Km in both the  $x$  and  $z$  directions. Periodic boundary conditions were imposed in both the  $x$  and  $z$  directions. The simulations run at a fixed time step of

$\Delta t = 5 \times 10^{-7}$  sec. and were terminated before the disturbances reach the simulation boundary. The grid resolution was selected to filter out the effect of whistler waves of frequencies above 100 kHz, consistent with the neglect of the electron mass and the displacement current.

In the simulations, a source current  $J_s$  with the form given by Eq. (2) was introduced into a spatial region filled with stationary plasma and uniform magnetic field  $B_0 = B_0 \hat{e}_z$ . This current source was located at the center of the simulation region, had a finite extent ( $L_s = 1$  Km) in  $x$ , and  $I_0 = 1$  mAmp/m. An equivalent three dimensional view of the source current is a thin current slab extending infinitely in the  $y$  direction. In the following, the current source will be simply referred to as the tether. Before presenting the results we make the following comments. First, the tether is introduced into the plasma region initially. This is equivalent to a current switch-on at time zero, with a rise time of one time step. Therefore, the timescale involved in the hybrid simulation favors the whistler excitation. Second, the assumption of quasi-neutrality in the hybrid code requires that there is no net charge accumulation in the simulation region. Therefore, the sheath phenomena around plasma contactors at the tether ends are not included. This is in consistent with the aim of this study which focuses on the current closure through magnetoplasma away from the sheath regions.

### Current Closure

Figure 1 shows the isomagnetic contours of the  $B_y$  field in the  $x$ - $z$  plane at times 0.1, 0.25, and 0.4 msec. Two dominant features can be distinguished. First, an oscillatory radiative structure propagates away from the tether in a characteristic whistler wavepacket with group velocity of  $v_g \approx 10^9$  cm/sec. Its wavefront spreads in a  $15 - 25^\circ$  cone with respect to  $B_0$ . This is followed by a region containing the bulk of magnetic field on either side of the tether. The bulk region is a localized magnetic field profile of the form  $\pm B_y(z \pm vt) \eta(|x| - L_s/2)$ . It expands spatially along  $B_0$  at a speed of  $v \approx v_g/2$  at early time, but the expansion slows down to  $v \ll v_g$  at late times. Dynamics of the bulk region is governed by the whistler portion of Eq. (1), which has the form of a diffusion equation

$$\partial B/\partial t + \nabla \times [(\nabla \times B) \times (cB_0/4\pi en_0)] = 0. \quad (3)$$

Thus, we can view the expansion as an analogous diffusion process which has a decreasing speed that asymptotes to zero as  $t \rightarrow \infty$ . The significance of the bulk of magnetic field around tether is that it embraces a region of substantial closure current. Since  $\nabla \times B = (4\pi/c) J$ , there is a cross-field current component  $J_x$  associated with the bulk region. As will be shown later,  $J_x$  is an essential component in the current closure path.

Figure 2 displays plots of  $B_x$  and  $B_y$  as functions of  $z$  along the line  $x = 0$ , at times 0.1, 0.25, and 0.4 msec. Notice that the early pulses of  $B_x$  and  $B_y$  exhibit typical characteristics of whistler waves. They are right-hand circularly polarized ( $B_x, B_y$

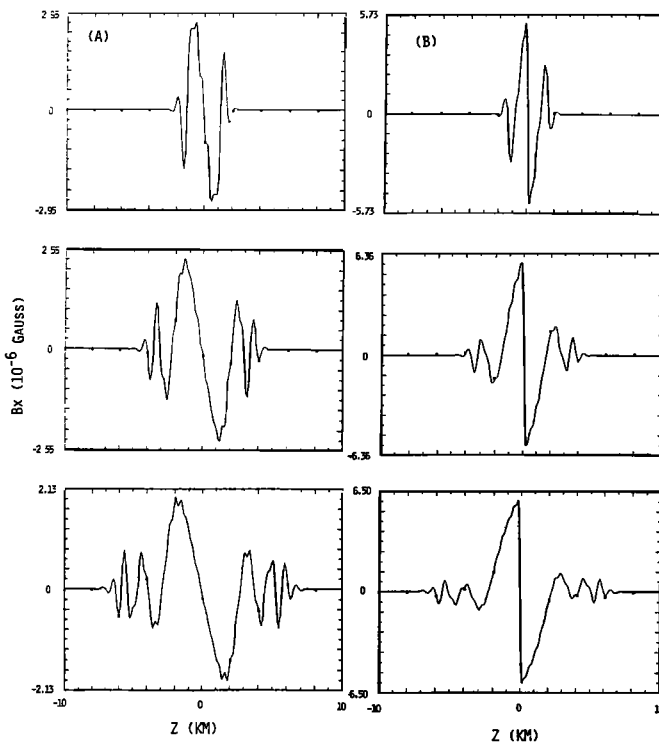
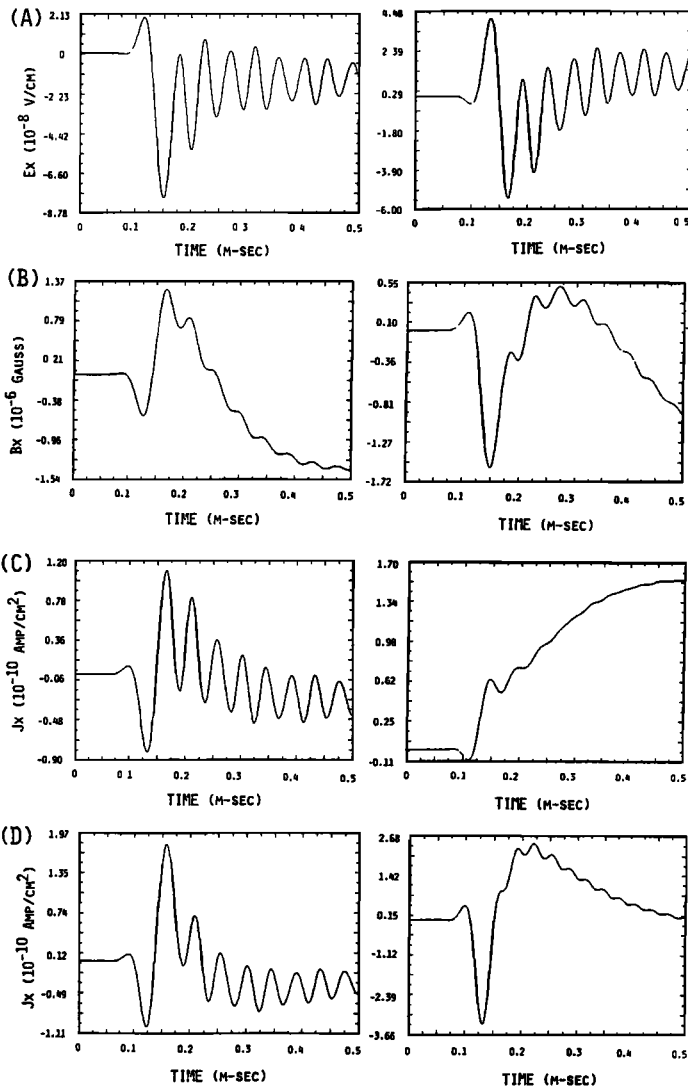


Figure 2. Cross section plots of field amplitude for (a)  $B_x(z)$ , and (b)  $B_y(z)$  along the midplane cutting across the center of the current source at  $x = 0$  and at times  $t = 0.1, 0.25,$  and  $0.4$  msec.



**Figure 3.** Field and current data at probe 1 & 2 as functions of time from  $t = 0$  to  $t = 0.5$  msec. Probe 1: row (a) electric fields  $E_x$  and  $E_y$ ; row (b) magnetic fields  $B_x$  and  $B_y$ ; and row (c) total plasma currents  $J_x$  and  $J_z$ .  $J_x$  and  $J_z$  at Probe 2 is in row (d).

90° out of the phase) and are highly dispersive, with shorter wavelengths running ahead of the longer ones. The wave amplitude approaches  $7 \times 10^{-6}$  G at the peak of the bulk, corresponding to a current strength of  $I_0 = 1$  mAmp/m in tether. Size of the bulk region, as is measured by the first node of  $B_y$ , increases incrementally from 1 km, 1.7 km, to 2.2 km at times 0.1, 0.25, and 0.4 msec, respectively. Therefore, the expansion of the bulk region is continuing during the simulation run and no steady state is yet reached.

To visualize the results two probes were introduced to monitor the temporal behavior of the current and of the fields. Probe 1 was located at (0.5 km, 2 km), on the magnetic field line passing through the end of the current source. Probe 2 was located at (0, 2km), on the midplane bisecting the current source. Time series data collected by probe 1 are shown in Figure 3. These data include the field components  $E_x$ ,  $E_y$ ,  $B_x$ ,  $B_y$ , and total current density components  $J_x$  and  $J_z$ . All the quantities are plotted as functions of time, from  $t = 0$  up to  $t = 0.5$  msec. The electric field plots in Figure 3(a) show an amplitude oscillation in time long after the pulse front caused by switch-on passes through the probe location. This indicates a continuous excitation and emission of whistler waves during the expansion of the current closure loop, even though the tether current is maintained at a steady value. The oscillation period is approximately 0.045

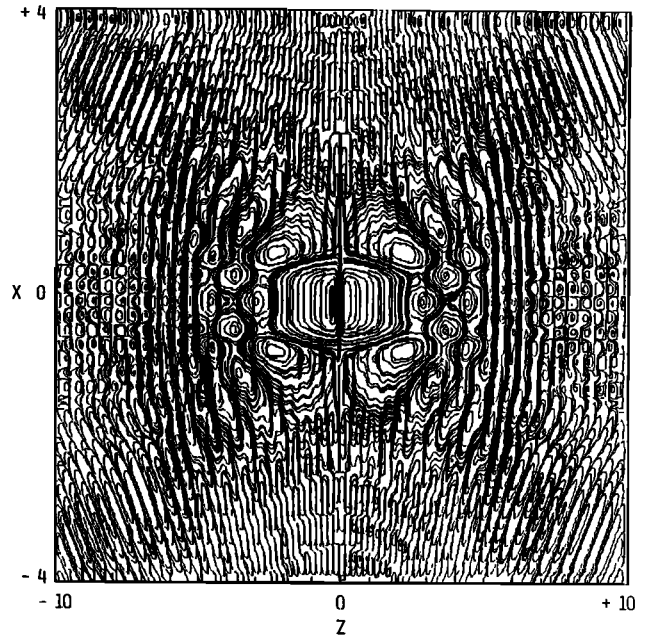


**Figure 4.** Streamline plot of the  $J_x$  versus  $J_z$  flow in the  $x$ - $z$  plane at a time  $t = 0.4$  msec.

msec, which corresponds to a wave frequency of 22 kHz. The oscillation phases of  $E_x$  and  $E_y$  are offset by one quarter of a time cycle (i.e. 90 degrees out of phase), again indicating that the emitted wave is indeed a right hand circularly polarized whistler wave. The magnetic field plots in Figure 3(b) show similar oscillations superimposed on a steadily growing amplitude in time after the pulse front passes through. Since the magnetic field is related to the plasma current through Ampere's law, the growing amplitude in  $B$  implies an increase in the plasma current around probe 1. The current components  $J_x$  and  $J_z$  are given in Figure 3(c). The  $J_z$  plot at the lower panel shows an initial jump as the pulse front arrives. This is followed by a monotonic amplitude increase that approaches a steady value at later time. Physically, this means that a field-aligned current starts to flow from the tip of the current source after switch-on. The current strength increases in time as the closure loop expands and asymptotes to a steady value. Accompanied with the formation of a field-aligned current  $J_z$  is the emergence of a cross-field current  $J_x$ . The left panel of Figure 3(c) shows an oscillatory behavior of  $J_x$  at early time and, by taking a time average over the oscillation period, the emergence of a net  $J_x$  component after

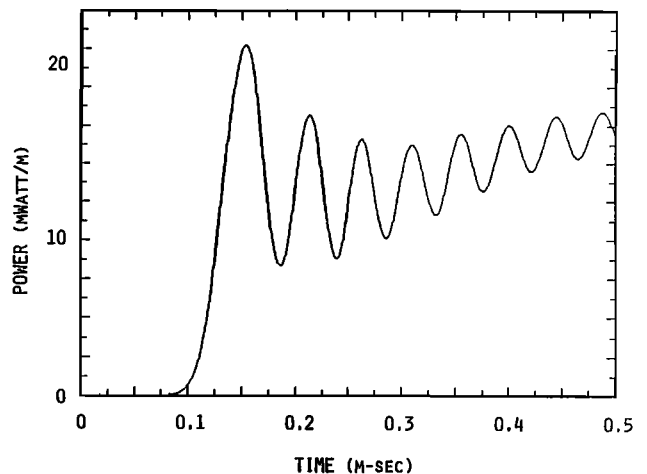


**Figure 5** Power loss due to whistler radiation along magnetic field line in the unit of mWatts/m, as a function of time.

0.3 msec. The amplitude of the net  $J_x$  current lies below the initial zero level, indicating that it flows in the  $-x$  direction.

Time series data collected by probe 2 show similar whistler emission characteristics as those in probe 1. However, probe 2 registers a net cross-field  $J_x$  current at late time as shown by Figure 3(d). The field-aligned current  $J_z$  behaves quite differently at late times also. Figure 3(d) shows that the  $J_z$  amplitude reaches a high level at the pulse front and falls toward zero afterward. This suggests that, as the closure loop expands way beyond probe 2, the only significant current component observed at mid-plane is the cross-field current  $J_x$ . The magnitude of the steady  $J_x$  is approximately the same as that at probe 1. Thus, the time-averaged  $J_x$  component constitutes the essential part of the current closure path through which the source current closes upon itself.

To complete the picture of current closure a 2D streamline plot of  $J_x$  versus  $J_z$  is provided in Figure 4. This is a snapshot taken at time  $t = 0.4$  msec, which shows that there is a region around the tether where streamlines connect to both ends of the current source. This region coincides with the bulk of the  $B_y$  region described in Figures 1-2 and can be viewed as the region for current closure since the tether current and the plasma currents form a closed loop. To be more exact, the complete current closure path consists of: (1) The outgoing portion of the closure current, as represented by the streamlines originating from the top of the tether along magnetic field lines connecting the top; (2) The cross-field portion of the closure current, as represented by the streamlines cutting across the magnetic field and the midplane on both sides of tether; and (3) The return portion of the closure current, as represented by the streamlines terminated at the bottom of the tether extending along magnetic field lines connecting the bottom. The transverse size of the closure region is estimated to be 2.2 km on either side of the tether at time  $t=0.4$  msec. Taking the expansion into account, the eventual closure circuit formed by the whistler pulses would be very localized.

### Radiation Loss

As noted above, continuous emission of whistler waves from the tether is observed while the current closure path forms and expands. This is most evident in Figure 3(a) and Figure 4(a), which show persistent oscillations in electric field amplitudes after the pulse front passes through the observation points. Power loss due to whistler radiation along a magnetic field line is estimated by integrating the Poynting flux across a constant  $z$  line passing through the diagnostic probes. Figure 5 shows the integrated Poynting flux, in units of mWatts/m, as a function of time. Total power loss due to whistler radiation asymptotes to a value of  $P = 32$  mWatts/m at late time. Note that this value is twice that given in the figure because whistler waves propagate in both directions of  $z$ . A set of simulations was conducted to find the scaling of radiation power as a function of the current strength  $I_0$ . It was found that electric field, magnetic field, electron flow speed, and density perturbation scale linearly with  $I_0$ , while the field energy densities and radiation power is proportional to the square of  $I_0$ . Therefore, a source current at ten times the present strength radiates at one hundred times the present power.

The radiation resistance  $R$  of the whistler circuit can be evaluated using the relation  $P = R I_0^2$ . Based on the values of  $P$  and  $I_0$  in unit length, the radiation resistance is estimated to be  $R = 3.2 \times 10^4$  Ohm/m. This numerical radiation resistance is two orders of magnitude larger than the analytic radiation resistance for the Alfvén waves [Dobrowolny and Veltri, 1986] based on a tether wire of 1 cm thick. Therefore, power loss due to whistler radiation is expected to be an important factor in determining the overall efficiency of the TSS. This agrees with an earlier analytical estimate by Barnett and Olbert [1986] who, using a constant-current moving-tether model, concluded that the radiation resistance from the lower hybrid band is much larger than that of the low frequency band.

### Discussion

The issues of the plasma response to an imposed cross-field current and its application to the TSS current closure have been addressed in this letter. Previous MHD studies [Drell et. al., 1965; Dobrowolny and Veltri, 1986] indicate that current closure is established by the Alfvénic pulse reaching the highly conducting lower ionosphere. In this scenario, a global current closure loop is envisioned and the timescale in forming such loop is expected to be longer than the ion cyclotron period [Goertz and Boswell, 1979]. Our simulation results augment previous understanding by focusing on closure processes of timescales shorter than the ion cyclotron period. Specifically, we consider the current closure being conducted by whistler-like processes in the magnetoplasma. In contrast to the Alfvénic picture, the whistler closure is highly localized around TSS and can be the dominant feature at early time. The Alfvénic processes can contribute to the current closure of the TSS only after the formation of the whistler loop. The details of the transition from the whistler closure to the Alfvénic one will be reported later.

**Acknowledgment.** This research was supported in part by NASA under contract NAS8-36811.

### References

- Banks, P. M., P. R. Williamson, and K.-I. Oyama, Electrical behavior of a shuttle electrodynamic tether system (SETS), *Planet. Space Sci.*, **29**, 139-147, 1981.
- Barnett, A., and S. Olbert, Radiation and waves by a conducting body moving through a magnetized plasma, *J. Geophys. Res.*, **91**, 10117-10135, 1986.
- Chapman, S., and V. C. A. Ferraro, A new theory of magnetic storm, *Terr. Mag.*, **36**, 77, 1931.
- Colombo, G., E. M. Gaposchkin, M. D. Grossi, and G. C. Weiffenbach, Shuttle-borne <<Sky-hook>>: a new tool for low orbital altitude research, Report Geoastronomy No. 1, Smithsonian Astrophysical Observatory, 1974.
- Dobrowolny, M., and P. Veltri, MHD power radiated by a large conductor in motion through a magnetoplasma, *Nuovo Cimento C*, **2**, 27-38, 1986.
- Drell, S. P., H. M. Foley, and M. A. Ruderman, Drag and propulsion of large satellites in the ionosphere: an Alfvén engine in space, *J. Geophys. Res.*, **70**, 3131-3145, 1965.
- Goertz, C.K., and R.W. Boswell, Magnetosphere-Ionosphere Coupling, *J. Geophys. Res.*, **84**, 7239-7246, 1979.
- Helliwell, R.A., *Whistlers and Related Ionospheric Phenomena*, p. 30, Stanford Univ. Press, 1965.
- Kokubun, S., K. Hayashi, H. Kawano, T. Yamamoto, A. Nishida, K. Shiokawa, Y. Tonegawa, F. Tohyama, and T. Kamei, Magnetic field measurements on GEOTAIL, AGU fall meeting, SM51C-9, 1992.
- Mankofsky, A., R. N. Sudan, and J. Denavit, Hybrid simulation of ion beams in background plasma, *J. Comp. Phys.*, **70**, 89-116, 1987.
- Papadopoulos, K., C. L. Chang, P. Vitello, and A. Drobot, On the efficiency of ionospheric ELF generation, *Radio Science*, **25**, 1311-1320, 1990.
- Stenzel, R.L., and J.M. Urrutia, Currents between tethered electrodes in a magnetized laboratory plasma, *J. Geophys. Res.*, **95**, 6209-6226, 1990.
- Urrutia, J.M., and R.L. Stenzel, Modeling of induced currents from electrodynamic tethers in a laboratory plasma, *Geophys. Res. Lett.*, **17**, 1589-1592, 1990.
- C. L. Chang, A. T. Drobot, and P. Satya-Narayana, Science Applications International Corporation, 1710 Goodridge Drive, McLean, Virginia 22102
- A. S. Lipatov, Institute of Space Physics, Moscow, Russia
- K. Papadopoulos, Department of Physics and Astronomy, University of Maryland, College Park, Maryland 20770

(Received: October 1, 1993; Revised: December 20, 1993; Accepted: February 28, 1994)